



Removal of disperse dye from aqueous solution using waste-derived activated carbon: Optimization study

A.A. Ahmad, B.H. Hameed*, A.L. Ahmad

School of Chemical Engineering, Engineering Campus, Universiti Sains Malaysia, 14300 Nibong Tebal, Penang, Malaysia

ARTICLE INFO

Article history:

Received 27 January 2009

Received in revised form 25 April 2009

Accepted 2 May 2009

Available online 18 May 2009

Keywords:

Rattan sawdust
Activated carbon
Adsorption
Disperse dye
Optimization

ABSTRACT

The purpose of this work is to obtain optimal preparation conditions for activated carbons prepared from rattan sawdust (RSAC) for removal of disperse dye from aqueous solution. The RSAC was prepared by chemical activation with phosphoric acid using response surface methodology (RSM). RSM based on a three-variable central composite design was used to determine the effect of activation temperature (400–600 °C), activation time (1–3 h) and H₃PO₄:precursor (wt%) impregnation ratio (3:1–6:1) on C.I. Disperse Orange 30 (DO30) percentage removal and activated carbon yield were investigated. Based on the central composite design, quadratic model was developed to correlate the preparation variables to the two responses. The most influential factor on each experimental design responses was identified from the analysis of variance (ANOVA). The optimum conditions for preparation of RSAC, which were based on response surface and contour plots, were found as follows: temperature of 470 °C, activation time of 2 h and 14 min and chemical impregnation ratio of 4.45.

© 2009 Elsevier B.V. All rights reserved.

1. Introduction

Activated carbons, with their high porosity, are extensively used in industrial purification and chemical recovery operations. This is due to their extended specific surface area between 500 and 2000 m²/g, their high pore volume and the presence of surface functional groups, especially oxygen groups [1]. Activated carbons are materials having complex porous structures with associated energetic as well as chemical inhomogeneities. Their structural heterogeneity is a result of existence of micropores, mesopores and macropores of different sizes and shapes. The main application of this adsorbent is for separation and purification of gaseous and liquid-phase mixtures [2].

A challenge in activated carbon production is to produce very specific carbons with a given pore size distribution from low-cost materials at low temperature. Precursors used for the production of activated carbons are organic materials that are rich in carbon, such as coal, lignite, and wood. Although coal is the most commonly used precursor, agricultural waste in certain condition is a better choice [3]. Many agricultural by-products such as coconut shell [4], grain sorghum [5], coffee bean husks [6], rubber wood sawdust [7], chestnut wood [8], fruit stones [9] and bamboo waste [10] have been discovered to be suitable precursors for activated carbon due to their high carbon and low ash contents. Agricultural wastes are

considered to be very important feedstock because of two basic facts: they are renewable sources and low-cost materials [11].

There are two processes for preparation of activated carbon: chemical activation and physical activation. Chemical activation is a single step method of preparation of activated carbon in the presence of chemical agents while physical activation involves carbonization of carbonaceous materials followed by activation of the resulting char in the presence of activating agents such as CO₂ or steam. The chemical activation usually takes place at a temperature lower than that used in physical activation; this results in an improvement of pore development in the carbon structure because of the effect of chemicals. The carbon yields of chemical activation are higher than physical one [12].

Rattan (Palmae/Arecaceae family) is spiny climbing plant belonging to the palm family. It is considered to be the most important non-wood forest product in Peninsular Malaysia. There are about 600 species in the world, of which 106 species are found in Peninsular Malaysia. Only 21 of these species, however, are utilized and marketed. Rattan also plays an important role in the manufacture of household commodities in many rural areas. In addition, value added rattan are utilized as furniture, walking sticks, rattan balls, baskets, toys and mats. Consequently considerable amount of sawdust are generated as residues. Currently most of these residues are used as boiler fuel. To make better use of rattan sawdust, it is proposed to convert it to an activated carbon. The advantage of using non-wood forest products as raw materials for manufacturing activated carbon is renewable and potentially less expensive [13]. Furthermore, preparation and characterization of adsorbent

* Corresponding author. Tel.: +60 4 599 6422; fax: +60 4 594 1013.
E-mail address: chbassim@eng.usm.my (B.H. Hameed).

Table 1
Independent variables and their coded levels for the central composite design.

Variables (factors)	Code	Unit	Coded variable levels				
			$-\alpha$	-1	0	$+1$	$+\alpha$
Temperature	X_1	(°C)	331.820	400	500	600	668.179
Activation time	X_2	(h)	0.318	1	2	3	3.681
Impregnation ratio (IR)	X_3	–	1.977	1:3	1:4.5	1:6	7.022

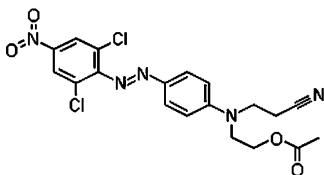
from rattan sawdust with H_3PO_4 activation are not available in the scientific literature.

The preparation of activated carbon is influenced by many factors such as temperature, time, and impregnation ratio. Therefore, it is important to study the effect of these factors on activated carbon production in order to determine the most important ones and their regions of interest [14]. Response surface methodology (RSM) is a useful tool to study the interactions of two or more factors. RSM is a collection of statistical and mathematical techniques useful for developing, improving and optimizing processes. It usually contains three stages: (i) design and experiments, (ii) response surface modeling through regression, (iii) optimization [15]. The main advantage of RSM is the reduced number of experimental trials needed to evaluate multiple parameters and their interactions [16]. In the last few years, RSM has been applied to optimize and evaluate interactive effects of independent factors in numerous chemical and biochemical processes. These applications are the preparation of activated carbons from olive-waste cakes by physical activation [17], sewage sludge by chemical activation [18] and Turkish lignite by chemical activation [14]. The focus of this research was to optimize the preparation conditions of activated carbon for removal of Disperse Orange 30 (DO30). A central composite design (CCD) was selected to study simultaneously the effects of three numerical activated carbon preparation variables: temperature, activation time and chemical impregnation ratio, on the two responses; percentage removal of DO30 and carbon yield.

2. Experimental

2.1. Adsorbate

C.I. Disperse Orange 30 (DO30), 4-((2,6-dichloro-4-nitrophenyl)azo)-N-(cyanoethyl)-N-(acetoxylethyl) supplied by Sigma-Aldrich (M) Sdn Bhd, Malaysia was used as an adsorbate. Distilled water was used to prepare all solutions. DO30 has a chemical formula of $C_{19}H_{17}Cl_2N_5O_4$, with molecular weight of 450.27 g/mol. The chemical structure of DO30 is as follows:



2.2. Preparation of activated carbon

The rattan sawdust was collected from a local furniture factory Penang, Malaysia. It was washed with hot distilled water to remove dust like impurities, dried at 105 °C until constant weight of the sample was reached and the material was finally sieved to discrete sizes. Chemical activation method using phosphoric acid (purity 85% Merck, Germany) was used to activate the raw material. 40 g of raw material was impregnated by certain amount of 40 wt% concentration phosphoric acid with occasional stirring. The amount of phosphoric acid solution used was adjusted to give a certain impregnation ratio (weight of activating agent:weight of precursor)

of 3:1, 4:1, 5:1, and 6:1. The impregnation ratio is given by

$$\text{impregnation ratio (IR)} = (\text{weight of } H_3PO_4 \text{ in solution}) : (\text{weight of precursor}) \quad (1)$$

After impregnation, the solution was filtered to take the residual acid. Subsequently, impregnated samples were air dried under sunlight for 3 days. Activation of phosphoric acid impregnated precursor was carried out at temperatures (400–600 °C) with a carbonization time of 1–3 h under nitrogen flow (150 cm³/g) at a heating rate of 10 °C/min. After activation, the samples were cooled to room temperature under nitrogen flow and were washed sequentially several times with hot distilled water (70 °C) until the washing solution attained pH of 6–7. Finally, the samples were oven dried at 110 °C for 24 h and then stored in plastic containers.

2.3. Design of experiment (DOE)

The RSM has several classes of designs, with its own properties and characteristics. Central composite design (CCD), Box-Behnken design and three-level factorial design are the most popular designs applied by the researchers. The CCD was used to study the effects of the variables towards their responses and subsequently in the optimization studies [19]. This method is suitable for fitting a quadratic surface and it helps to optimize the effective parameters with a minimum number of experiments, as well as to analyze the interaction between the parameters. In order to determine if there exist a relationship between the factors and the response variables investigated, the data collected must be analyzed in a statistically manner using regression. A regression design is normally employed to model a response as a mathematical function (either known or empirical) of a few continuous factors and good model parameter estimates are desired [19]. In developing the regression equation, the test factors were coded according to Eq. (2):

$$x_i = \frac{X_i - X_i^x}{\Delta X_i} \quad (2)$$

where x_i is the coded value of the i th independent variable, X_i the natural value of the i th independent variable, X_i^x the natural value of the i th independent variable at the center point, and ΔX_i is the value of step change.

Each response was used to develop an empirical model that correlated the response to the activated carbon preparation variables using a second-degree polynomial equation as given by Eq. (3) [19]:

$$Y = b_0 + \sum_{i=1}^n b_i x_i + \left(\sum_{i=1}^n b_{ii} x_i \right)^2 + \sum_{i=1}^{n-1} \sum_{j=i+1}^n b_{ij} x_i x_j \quad (3)$$

where Y is the predicted response, b_0 the constant coefficient, b_i the linear coefficients, b_{ij} the interaction coefficients, b_{ii} the quadratic coefficients and x_i , x_j are the coded values of the activated carbon preparation variables.

The ranges and the levels of the variables investigated in the study are given in Table 1. The experimental sequence was randomized in order to minimize the effects of the uncontrolled factors. The responses were percentage removal on DO30 (Y_1) and activated

Table 2
Experimental factors in coded units and experimental responses.

Run no.	Type	X ₁ : temp. code	X ₂ : time code	X ₃ : IR code	Temperature (°C)	Time (h)	IR	Percentage removal, Y ₁ (%)	Carbon yield, Y ₂ (%)
1	Axial	0	0	1.682	500	2	7.022	51.04	24.65
2	Center	0	0	0	500	2	4.5	72.79	32.76
3	Factorial	1	-1	-1	600	1	3	51.04	26.12
4	Axial	-1.682	0	0	331.820	2	4.5	33.57	42.43
5	Axial	1.682	0	0	668.179	2	4.5	55.57	10.75
6	Factorial	1	1	-1	600	3	3	46.68	13.51
7	Axial	0	0	-1.682	500	2	1.977	34.79	33.86
8	Factorial	1	-1	1	600	1	6	49.24	31.83
9	Factorial	-1	-1	1	400	1	6	32.55	37.07
10	Factorial	-1	1	-1	400	3	3	43.48	26.71
11	Center	0	0	0	500	2	4.5	77.04	29.54
12	Axial	0	-1.682	0	500	0.318	4.5	27.24	40.75
13	Center	0	0	0	500	2	4.5	78.02	27.75
14	Factorial	1	1	1	600	3	6	58.77	11.98
15	Center	0	0	0	500	2	4.5	76.79	27.98
16	Center	0	0	0	500	2	4.5	71.43	28.82
17	Axial	0	1.682	0	500	3.681	4.5	65.58	19.87
18	Factorial	-1	1	1	400	3	6	49.82	26.67
19	Center	0	0	0	500	2	4.5	74.87	28.31
20	Factorial	-1	-1	-1	400	1	3	36.64	41.55

carbon yield (Y₂). Each response was used to develop an empirical model that correlated the response to the activated carbon preparation variables using a second-degree polynomial equation as given by Eq. (3).

2.4. Model fitting and statistical analysis

The regression and graphical analysis with statistical significance were done using Design-Expert software (version 6.0.6, Stat-Ease, Inc., Minneapolis, USA). In order to visualize the relationship between the experimental variables and responses, the response surface and contour plots were generated from the models. The optimum values of the process variables were obtained from the response surface.

2.5. Adsorption studies

Batch adsorption was performed in 20 sets of 250 mL Erlenmeyer flasks where 100 mL of DO30 solution with initial dye concentration of 100 mg/L was placed in each flask. The pH of the solution was not adjusted. 0.30 g of each of the prepared activated carbon, with particle size of 200–300 μm was added to each flask and kept in a thermostated shaker of 120 rpm at 30 °C until equilibrium was reached. Aqueous samples were taken from the solutions and the concentrations were analyzed. The concentrations of DO30 in the supernatant solutions before and after adsorption were determined using a double beam UV–vis spectrophotometer (UV-1601 Shimadzu, Japan) at its maximum wavelength of 425.5 nm. The dye percentage removal can be calculated as follows:

$$\text{percentage removal} = \frac{C_0 - C_e}{C_0} \times 100 \quad (5)$$

where C₀ and C_e (mg/L) are the liquid-phase concentrations of dye at initial and equilibrium, respectively.

2.6. Activated carbon yield

The activated carbon yield was calculated based on Eq. (6).

$$\text{yield (\%)} = \frac{w_c}{w_o} \times 100 \quad (6)$$

where w_c (g) is the dry weight of final activated carbon and w_o (g) is the dry weight of precursor.

2.7. Characterization of activated carbon

The surface area and pore size were measured by N₂ adsorption isotherm using an ASAP 2020 Micromeritics instrument and by Brunauer–Emmett–Teller (BET) method.

The surface functional group of the RSAC was detected by Fourier Transform Infrared (FTIR) spectroscope (FTIR-2000, PerkinElmer). The spectra were recorded from 4000 to 400 cm⁻¹.

Scanning electron microscopy analysis was carried out on the precursor, precursor impregnated with H₃PO₄ and RSAC. The sample was placed on the aluminium tub and coated with gold for electron reflection. The sample was then vacuumed for 5–10 min prior to analysis.

Elemental analysis was performed using Elemental Analyzer (PerkinElmer, Series II, 2400) to investigate the presence of elements of carbon, hydrogen, and nitrogen in precursor and RSAC. The content of sulphur and oxygen was determined from the difference of the total carbon, hydrogen, and nitrogen composition.

3. Results and discussion

3.1. Experimental design

The CCD consists of a 2ⁿ factorial runs with 2n axial runs and nc center runs (six replicates). In the present study, the activated carbons were prepared using chemical activation method by varying the preparation variables using the CCD. The variables studied were activation temperature (X₁), activation time (X₂) and H₃PO₄ impregnation ratio (X₃). These three variables together with their respective ranges were chosen based on the literature and preliminary studies. Activation temperature, activation time and chemical impregnation ratio were found to be important parameters affecting the characteristics of the activated carbons produced [12,20–22]. For each variable, a 2³ full factorial CCD for the three variables consisting of eight factorial points, six axial points and six replicates at the center points were employed, indicating that altogether 20 experiments were required, as calculated from Eq. (7) [23]:

$$N = 2^n + 2n + nc = 2^3 + 2 \times 3 + 6 = 20 \quad (7)$$

where N is the total number of experiments required and n is the number of factors.

The center points are used to determine the experimental error and the reproducibility of the data. The independent vari-

Table 3
Analysis of variance (ANOVA) and lack-of-fit test for response surface quadratic model for percentage removal.

Source	Sum of squares	Degree of freedom (DF)	Mean square	F-Value	Prob > F	Comment
Model	5055.22	9	561.6913	18.28576	<0.0001	Significant
X_1	471.439	1	471.4386	15.3476	0.0029	
X_2	116.392	1	116.3919	3.789119	0.0802	
X_3	643.701	1	643.7006	20.95556	0.0010	
X_1^2	1478.47	1	1478.469	48.1313	<0.0001	
X_2^2	1294.65	1	1294.652	42.14718	<0.0001	
X_3^2	1654.22	1	1654.224	53.85297	<0.0001	
X_1X_2	44.8405	1	44.84045	1.459773	0.2548	
X_1X_3	8.0802	1	8.0802	0.26305	0.6192	
X_2X_3	73.9328	1	73.9328	2.406869	0.1519	
Residual	307.174	10	30.71741			
Lack-of-fit	273.189	5	54.63788	8.038592	0.0196	Significant
Pure error	33.9847	5	6.796947			

$R^2 = 0.942$; Adj $R^2 = 0.891$.

Table 4
Analysis of variance (ANOVA) and lack-of-fit test for response surface quadratic model for carbon yield.

Source	Sum of squares	Degree of freedom (DF)	Mean square	F-Value	Prob > F	Comments
Model	1450.713	9	161.190	14.810	0.0001	Significant
X_1	759.415	1	759.415	69.775	<0.0001	
X_2	18.347	1	18.3473	1.686	0.2233	
X_3	630.802	1	630.803	57.958	<0.0001	
X_1^2	24.045	1	24.0457	2.209	0.1680	
X_2^2	0.0079	1	0.0079	0.0007	0.9790	
X_3^2	1.760	1	1.7603	0.1617	0.6960	
X_1X_2	6.516	1	6.516	0.5986	0.4570	
X_1X_3	9.461	1	9.461	0.869	0.3731	
X_2X_3	0.98	1	0.98	0.090	0.7703	
Residual	108.836	10	10.884			
Lack-of-fit	91.521	5	18.304	5.285	0.0458	Significant
Pure error	17.3163	5	3.463			

$R^2 = 0.930$; Adj $R^2 = 0.867$.

ables are coded to the $(-1, 1)$ interval where the low and high levels are coded as -1 and $+1$, respectively. The axial points are located at $(\pm\alpha, 0, 0)$, $(0, \pm\alpha, 0)$ and $(0, 0, \pm\alpha)$ where α is the distance of the axial point from center and makes the design rotatable. In this study, α value was fixed at 1.682 (rotatable). The experimental sequence was randomized in order to minimize the effects of the uncontrolled factors. The two responses were DO30 percentage removal (Y_1) and activated carbon yield (Y_2). The complete design matrixes of the experiments carried out, together with the results obtained, are shown in Table 2.

3.2. Analysis of variance

The adequacy of the models was further justified through analysis of variance (ANOVA). The ANOVA for the quadratic model for DO30 percentage removal is listed in Table 3. The Model F -value of 19.66 implied that the model was significant as well. Values of $\text{Prob} > F$ less than 0.05 indicated that the model terms were significant. In this case, X_1^2 , X_2^2 and X_3^2 were significant model terms whereas the interaction terms X_1X_2 , X_1X_3 , X_2X_3 were all insignificant to the response. The ANOVA for the quadratic model for activated carbon yield is listed in Table 4. From the ANOVA for response surface quadratic model for yield, the Model F -value of 14.810 implied that the model was significant. In this case, activation temperature X_1 and impregnation ratio X_3 were significant model terms whereas X_2 , X_1^2 , X_2^2 , X_3^2 and X_1X_2 , X_1X_3 , X_2X_3 were insignificant model terms. From the statistical results obtained, it was shown that the above models were adequate to predict the adsorption capacity and the yield within the range of variables studied. $\text{Prob} > F$ is the probability that the variation in the results are due to random error and thus the very low values obtained

for the two models (<0.0001) indicate that results are not random and the terms in the models have a significant effect in the response.

3.3. Lack-of-fit test

Lack-of-fit is a special diagnostic test for adequacy of a model that compares the pure error, based on the replicate measurements to the other lack of fit, based on the model performance [24]. F -Value, calculated as the ratio between the lack-of-fit mean square and the pure error mean square, is the statistic parameter used to determine whether the lack-of-fit is significant or not, at a significance level α . In this case, the percentage removal and the carbon yield probability $> F$ values are 0.0206 and 0.0458, respectively revealing a desirable significant lack of fit.

3.4. Process models

By using multiple regression analysis, the responses (percentage removal and the carbon yield) were correlated with the three variables studied using the second-order polynomial as represented by Eq. (3). The coefficients of the model equation and their statistical significance were evaluated using Design-Expert 6.0.6 software. The quadratic regression model for the percentage removal and carbon yield in terms of coded factors are given by Eqs. (8) and (9), respectively:

(%) Percentage removal:

$$Y_1 = 75.05 + 5.88X_1 + 6.87X_2 + 2.92X_3 - 10.13X_1^2 - 9.48X_2^2 - 10.71X_3^2 - 2.37X_1X_2 + 1.01X_1X_3 + 3.04X_2X_3 \quad (8)$$

(%) Carbon yield:

$$Y_2 = 29.25 - 7.46X_1 - 6.80X_2 - 1.16X_3 - 1.30X_1^2 + 0.023X_2^2 - 0.35X_3^2 - 0.90X_1X_2 + 1.09X_1X_3 - 0.35X_2X_3 \quad (9)$$

where X_1 , X_2 and X_3 are the coded values of the process variables activation temperature, activation time and chemical impregnation ratio, respectively. The coefficients with one factor represent the effect of the particular factor, while the coefficients with two factors and those with second-order terms represent the interaction between the two factors and quadratic effect, respectively. The positive sign in front of the terms indicates synergistic effect, while negative sign indicates antagonistic effect.

The statistical analysis gives several comparative measures for the model selection. Ignoring the aliased model, the quadratic model seems to be the best: based on low standard deviation and high R^2 statistics. The value of R^2 for the percentage removal and carbon yield were 0.942 and 0.930, respectively. This is also evident from the fact that the plot of predicted versus experimental percentage removal and carbon yield in Fig. 1(a) and (b) are close to showing that the prediction of experimental data is quite satisfactory. These plots therefore visualize the performance of the model.

3.5. Effects of process variables

The graphical representations of the models (Eqs. (8) and (9)) facilitate an examination of the effects of the experimental factors on the responses, 3D surface graphs and contour plots between the factors were obtained using the Design-Expert software and are presented in Figs. 2 and 3, respectively. These figures illustrate the responses of different experimental variables and can be used to identify the major interactions between the variables. The 3D surface graph and contour plot in Fig. 2 show that the DO30 percentage removal (Y_1) increased with the increase in activation temperature and chemical impregnation ratio. The activation time was fixed at zero level. The response surface in Fig. 2 shows a curvature. These indicate that the interaction effect between activation temperature and chemical impregnation ratio on percentage removal is greatly pronounced, as confirmed by significance test. The results obtained were in agreement with the work of Sudaryanto et al. [12] which reported that activation time gave no significant effect on the pore structure of activated carbon produced from cassava peel, and the pore characteristics changed significantly with the activation temperature and also the KOH impregnation ratio. Sentorun-Shalaby et al. [25] also found that activation time did not show much effect on the surface area obtained for activated carbons prepared from apricot stones using steam activation. However, in this work, all the three variables studied were found to have synergistic effects on the adsorption capacity of the activated carbons prepared.

Fig. 3 shows the effect of activation temperature and impregnation ratio on the carbon yield (activation time was fixed at zero level). The carbon yield was found to decrease with increasing temperature, activation time and chemical impregnation ratio. The highest yield was obtained when all the three variables were at the minimum point within the range studied. Fig. 3 for carbon yield (Y_2) on the other hand, temperature was found to have the greatest effect on it, while activation time and chemical impregnation ratio were less significant compared to temperature. However, the interaction effects between the variables were less significant. The effects of temperature and chemical impregnation ratio on yield were studied as they were found to have significant effects on the response. This result was in agreement with the work done by Hameed et al. [26] which found that activation temperature played an important role on the yield of oil palm fibre-based activated

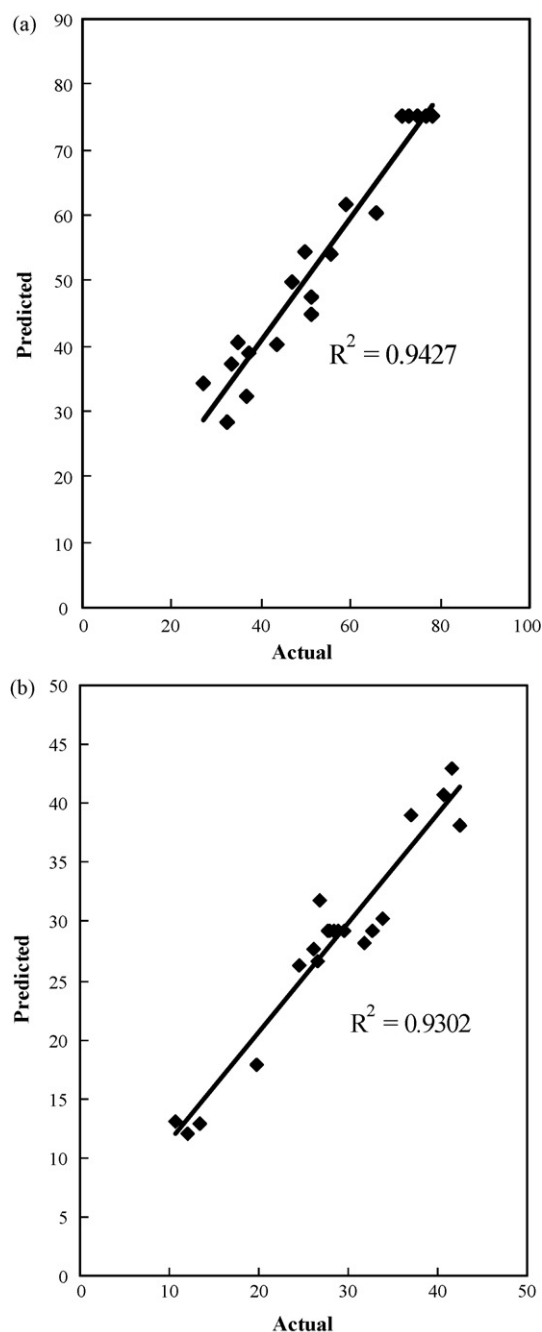


Fig. 1. Predicted vs. actual data for (a) percentage removal and (b) carbon yield.

carbon whereas activation time did not show much effect on the carbon yield. The yield was strongly affected by the activation temperature, where increasing activation temperature decreased the yield and increased the carbon burn off. This was because when higher activation temperature was used, the weight losses were due to increase evolution of volatile matters from the precursor, leading to increase of the pore development, and creates new pores, as a result of intensifying dehydration and elimination reactions [27].

3.6. Optimization analysis

The experimental conditions with the function of desirability were applied using Design-Expert software version 6.0.6 (STAT-EASE Inc., Minneapolis, USA). The experiments were conducted at these conditions and comparison between the experimental results

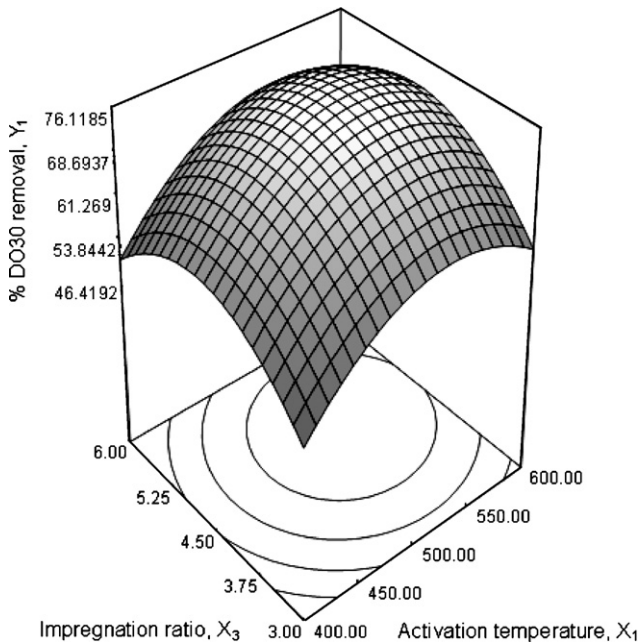


Fig. 2. Effect of activation temperature and chemical impregnation ratio on percentage removal; 3D surface graph and contour plot.

with the predicted results from the model was made. The optimum activated carbon prepared from rattan sawdust was obtained by using temperature of 470 °C, activation time of 2 h and 14 min and chemical impregnation ratio of 4.45. At the optimum condition, the DO30 removal and activated carbon yield were found to be 75.102% and 33.094%, respectively. However, the experimental values obtained at optimum condition for DO30 removal and activated carbon yield were found to be 69.735% and 30.213%, respectively. It was observed that the experimental values obtained were in good agreement with the values predicted from the models, with relatively small errors between the predicted and the experimental values, which were only 7.15% and 8.71%, respectively for DO30

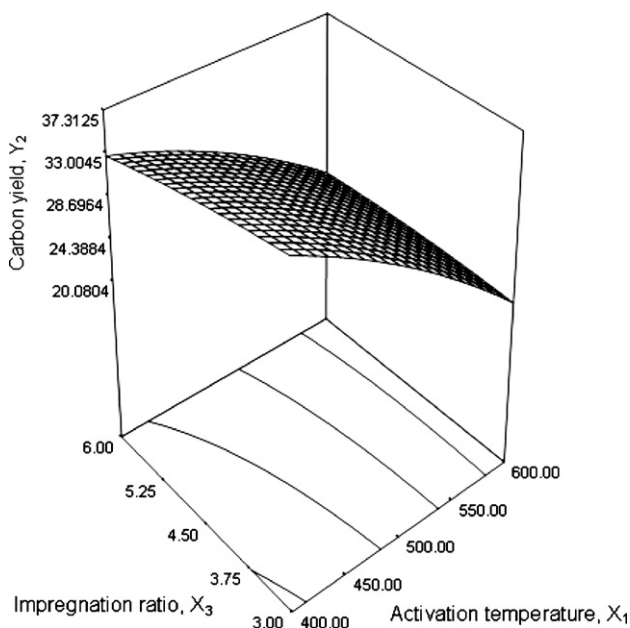


Fig. 3. Effect of activation temperature and chemical impregnation ratio on carbon yield; 3D surface graph and contour plot.

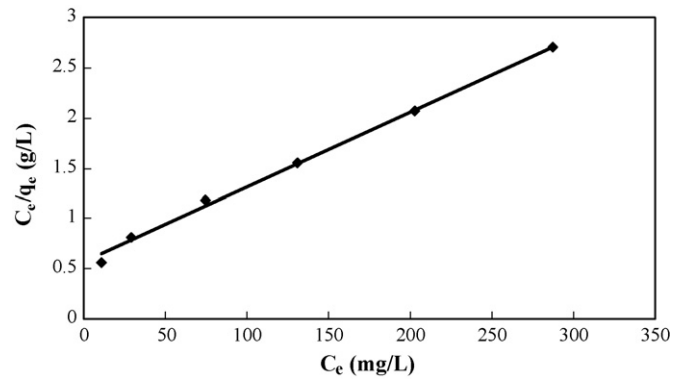


Fig. 4. Langmuir adsorption isotherm of DO30 on rattan sawdust-based activated carbon prepared under optimum condition at 30 °C.

removal and activated carbon yield. This result agrees with the work done by Amina et al. [28].

3.7. Adsorption isotherm of DO30 on activated carbon prepared under optimum condition

The DO30 adsorption capacity of the activated carbon prepared under optimum conditions was determined by performing adsorption tests in a set of 250 mL Erlenmeyer flasks where 100 mL of DO30 solutions with initial concentrations of 50–500 mg/L were placed in these flasks. Other operating parameters such as activated carbon dosage, solution temperature and agitation speed were similar to the adsorption studies carried out for determining the DO30 uptake. The amount of adsorption at equilibrium, q_e (mg/g) was calculated from the following equation:

$$q_e = \frac{(C_o - C_e)V}{W} \tag{10}$$

where q_e (mg/g) is the amount of dye adsorbed at equilibrium, C_o and C_e (mg/L) are the liquid-phase concentrations of dye at initial and equilibrium, respectively. V (L) is the volume of the solution, and W (g) is the mass of dry adsorbent used.

The adsorption data obtained were then fitted to the Langmuir isotherm model to determine the DO30 adsorption capacity of the activated carbon prepared. Besides, from literatures, most of the equilibrium data obtained for adsorption of dyes on activated carbons were found to be best represented by the Langmuir model [21,29,30]. Langmuir [31] isotherm assumes monolayer adsorption onto a surface containing a finite number of adsorption sites of uniform strategies of adsorption with no transmigration of adsorbate in the plane on surface. The linear form of Langmuir isotherm equation is given as

$$\frac{C_e}{q_e} = \frac{1}{q_{max}K_L} + \frac{C_e}{q_{max}} \tag{11}$$

where C_e (mg/L) is the equilibrium concentration of the adsorbate, q_e (mg/L) is the amount of adsorbate adsorbed per unit mass of adsorbent, q_{max} (mg/g) is the maximum amount of the adsorbate per unit weight of the adsorbent to form a complete monolayer on the surface whereas K_L (L/mg) is Langmuir constant related to the affinity of the binding sites. When C_e/q_e was plotted against C_e , a straight line with slope of $1/q_{max}$ was obtained, as shown in Fig. 4. The q_{max} and K_L were 133.33 mg/g and 0.0133 L/mg, respectively. The correlation coefficient, R^2 value of 0.996 indicated that the adsorption data of DO30 on the activated carbon prepared were well represented by the Langmuir isotherm.

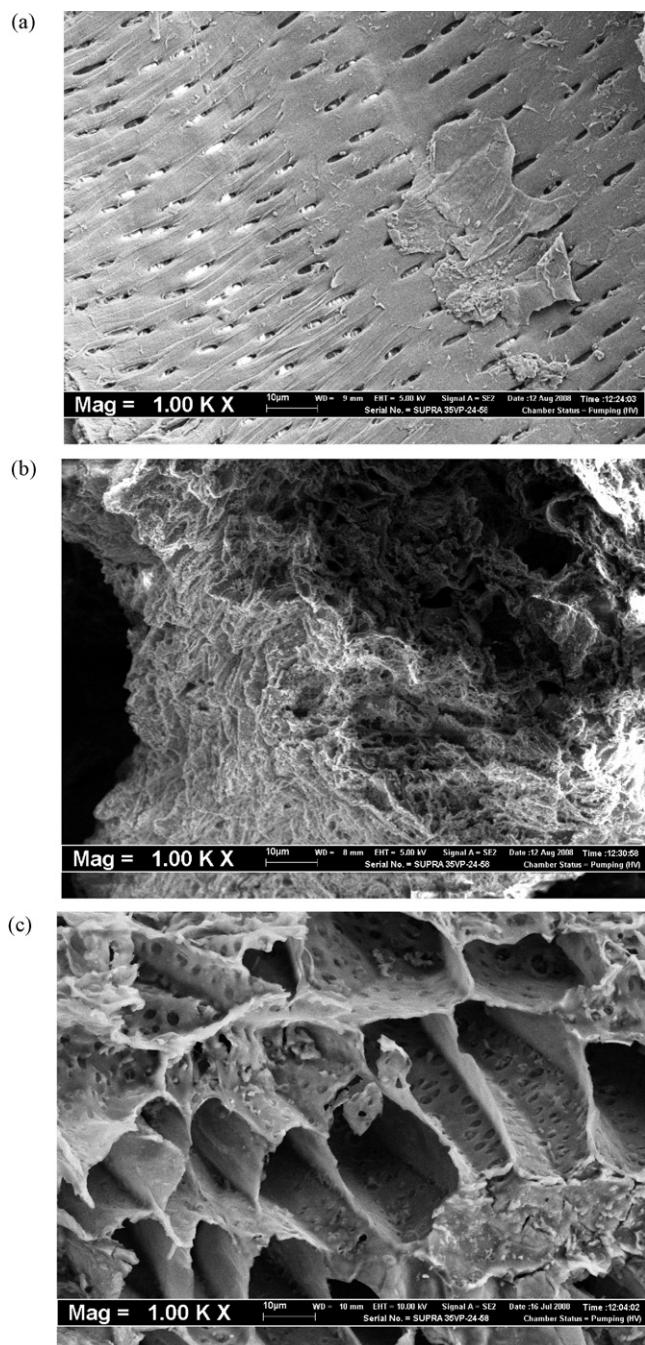


Fig. 5. Scanning electron micrograph: (a) precursor, (b) precursor impregnated with H_3PO_4 (impregnation ratio is 1:4.5) and (c) RSAC prepared under optimum condition (magnification: 1000 \times).

3.8. Characterization of the optimally prepared activated carbon

3.8.1. BET surface area and pore volume

The BET surface area of the prepared activated carbon was found to be 1037.18 m^2/g and Langmuir surface area 1621.42 m^2/g with total pore volume of 0.664 cm^3/g . The average pore diameter was found to be 2.56 nm. The high BET surface area, total pore volume and pore developments of the prepared activated carbon were due to the activation process using H_3PO_4 as chemical activating agent. The chemical agents are dehydrating agents that penetrate deep into the structure of the carbon causing pores to develop [32]. Besides, the average pore diameter of 2.56 nm indicates that the

activated carbon prepared was in the mesopores region according to the IUPAC classification [33].

3.8.2. Surface chemistry

The FTIR spectra of the optimally rattan sawdust activated carbon displayed the following bands (figure is not shown): 3435 cm^{-1} (O–H stretching vibrations), 2302 cm^{-1} (C=O stretching from ketones, aldehydes or carboxylic groups), 1620 cm^{-1} (C=O stretching in quinones or carboxylic anhydrides) and 808 cm^{-1} (C–H out-of-plane bending in benzene derivatives). The main surface functional groups present in the derived activated carbon were quinone and aromatic rings. The stretching vibrations found was probably due to the incorporation of heteroatoms at the edge of the aromatic sheet or within the carbon matrix [34]. The FTIR spectra obtained was in agreement with the results reported in the studies carried out on activated carbons prepared from rice straws [35] and cherry stones [36].

3.8.3. Surface morphology

Fig. 5(a), (b) and (c), respectively shows the SEM images of the precursor (raw rattan sawdust), precursor impregnated with H_3PO_4 and the RSAC obtained under the optimum preparation conditions. As can be seen from Fig. 5(a) there is few pores available on the surface of the precursor. Fig. 5(b) shows that impregnation of precursor with H_3PO_4 was effective in creating pores on the surfaces of the precursor. Fig. 5(c) shows that the chemical activation process was effective in creating well-developed pores on the surfaces of the activated carbon leading to the activated carbon with large surface area and porous structure. Similar observations were reported by other researchers in their works of preparing activated carbons from apricot stones [27] and pistachio-nut shells [37].

3.8.4. Elemental analysis

The elemental analysis of the precursor and activated carbon prepared under the optimum condition indicated that the percentage of C, H, N and others found in the precursor and activated carbon were 44.93%, 5.23%, 0.10% and 49.74% for precursor and 74.86%, 2.87%, 0.40% and 21.87% for activated carbon. Both samples have moderate nitrogen content, less than 1%, but noteworthy oxygen content (in others) which does not follow a specific trend with increasing sample burn-off.

4. Conclusion

Response surface methodology was used to evaluate the effects of temperature, activation time and chemical impregnation ratio, on the percentage removal on DO30 and carbon yield. The adequacy of the quadratic model was verified effectively by the validation of experimental data. The optimum results showed that the percentage removal of DO30 69.735% and carbon yield 30.21%. Process optimization was carried out and the experimental values obtained for the percentage removal and yield were found to agree satisfactory with the predicted values. Additionally, through analysis of the response surfaces derived from the models, activation temperature and chemical impregnation ratio were found to have significant effects on activated carbon yield compared to activation time whereas activation temperature showed the most significant effect on activated carbon yield. The R^2 values of the response parameters show a good fit of the models with experimental data. The activated carbon prepared under the optimum conditions were found to have well-developed pores on its surface. From the SEM image obtained, large and well-developed pores were clearly found on the surface of the activated carbon. The BET surface area of the prepared activated carbon was 1037.18 m^2/g and various functional groups on the prepared activated carbon were determined from

the FTIR results. The equilibrium data were well represented by the Langmuir isotherm, giving maximum monolayer adsorption capacity as high as 133 mg/g at 30 °C.

Acknowledgement

The authors acknowledge the research grant provided by the Universiti Sains Malaysia under the Research University (RU) Scheme (Project No. 1001/PJKIMIA/814005).

References

- [1] R.C. Bansal, J.B. Donnet, F. Stoeckli, *Active Carbon*, Marcel Dekker, New York, 1988.
- [2] S. Ismadji, S.K. Bhatia, Characterization of activated carbons using liquid phase adsorption, *Carbon* 39 (2001) 1237–1250.
- [3] D. Prahaz, Y. Kartika, N. Indraswati, S. Ismadji, Activated carbon from jackfruit peel waste by H₃PO₄ chemical activation: pore structure and surface chemistry characterization, *Chem. Eng. J.* 140 (2008) 32–42.
- [4] Z. Hu, M.P. Srinivasan, Preparation of high-surface-area activated carbons from coconut shell, *Micropor. Mesopor. Mater.* 27 (1999) 11–18.
- [5] Y. Diao, W.P. Walawender, L.T. Fan, Activated carbons prepared from phosphoric acid activation of grain sorghum, *Bioresour. Technol.* 81 (2002) 45–52.
- [6] M.C. Baquero, L. Giraldo, J.C. Moreno, F. Suarez-Garcia, A. Martinez-Alonso, J.M.D. Tascon, Activated carbons by pyrolysis of coffee bean husks in presence of phosphoric acid, *J. Anal. Appl. Pyrol.* 70 (2003) 779–784.
- [7] C. Srinivasakannan, M.Z.A. Bakar, Production of activated carbon from rubber wood sawdust, *Biomass Bioenergy* 27 (2004) 89–96.
- [8] V. Gomez-Serrano, E.M. Cuerda-Correa, M.C. Fernandez-Gonzales, M.F. Alexandre-Franco, A. Macias-Garcia, Preparation of activated carbons from chestnut wood by phosphoric acid—chemical activation, study of microporosity and fractal dimension, *Mater. Lett.* 59 (2005) 846–853.
- [9] A.M. Puzi, O.I. Poddubnaya, A. Martinez-Alonso, F. Suarez-Garcia, J.M.D. Tascon, Surface chemistry of phosphorus-containing carbons of lignocellulosic origin, *Carbon* 43 (2005) 2857–2868.
- [10] B.H. Hameed, A.T.M. Din, A.L. Ahmad, Adsorption of methylene blue onto bamboo-based activated carbon: kinetics and equilibrium studies, *J. Hazard. Mater.* 141 (2007) 819–825.
- [11] G.G. Stavropoulos, A.A. Zabaniotou, Production and characterization of activated carbons from olive-seed waste residue, *Micropor. Mesopor. Mater.* 83 (2005) 79–85.
- [12] Y. Sudaryanto, S.B. Hartono, W. Irawaty, H. Hindarso, S. Ismadji, High surface area activated carbon prepared from cassava peel by chemical activation, *Bioresour. Technol.* 97 (2006) 734–739.
- [13] B.H. Hameed, L.H. China, S. Rengarajb, Adsorption of 4-chlorophenol onto activated carbon prepared from rattan sawdust, *Desalination* 225 (2008) 185–198.
- [14] F. Karacan, U. Ozden, S. Karacan, Optimization of manufacturing conditions for activated carbon from Turkish lignite by chemical activation using response surface methodology, *Appl. Therm. Eng.* 27 (2007) 1212–1218.
- [15] R.H. Myers, D.C. Montgomery, *Response Surface Methodology: Process and Product Optimization Using Designed Experiments*, first ed., John Wiley and Sons Inc., New York, 1995.
- [16] J. Lee, L. Ye, W.O. Landen, R.R. Eitenmiller, Optimization of an extraction procedure for the quantification of vitamin E in tomato and broccoli using response surface methodology, *J. Food Compos. Anal.* 13 (2000) 45–57.
- [17] A. Bacaoui, A. Yaacoubi, A. Dahbi, C. Bennouna, R.P.T. Luu, F.J. Maldonado-Hodar, J. Rivera-Utrilla, C. Moreno-Castilla, Optimization of conditions for the preparation of activated carbons from olive-waste cakes, *Carbon* 39 (2001) 425–432.
- [18] S. Rio, F.B. Catherine, C.L. Le, C. Philippe, P.L. Cloirec, Experimental design methodology for the preparation of carbonaceous sorbents from sewage sludge by chemical activation—application to air and water treatments, *Chemosphere* 58 (2005) 423–437.
- [19] D.C. Montgomery, *Design and Analysis of Experiments*, fifth ed., John Wiley and Sons Inc., New York, USA, 2001.
- [20] G.G. Stavropoulos, A.A. Zabaniotou, Production and characterization of activated carbons from olive-seed waste residue, *Micropor. Mesopor. Mater.* 82 (2005) 79–85.
- [21] J.H. Tay, X.G. Chen, S. Jeyaseelan, N. Graham, Optimising the preparation of activated carbon from digested sewage sludge and coconut husk, *Chemosphere* 44 (2001) 45–51.
- [22] F.C. Wu, R.L. Tseng, Preparation of highly porous carbon from fir wood by KOH etching and CO₂ gasification for adsorption of dyes and phenols from water, *J. Colloid Interface Sci.* 294 (2006) 21–30.
- [23] R. Azargohar, A.K. Dalai, Production of activated carbon from Luscar char: experimental and modelling studies, *Micropor. Mesopor. Mater.* 85 (2005) 219–225.
- [24] M.Y. Noordin, V.C. Venkatesh, S. Sharif, S. Elting, A. Abdullah, Application of response surface methodology in describing the performance of coated carbide tools when turning AISI 1045 steel, *J. Mater. Process. Technol.* 145 (1) (2004) 46–58.
- [25] C. Sentorun-Shalaby, M.G. Ucak-Astarlioglu, L. Artok, C. Sarici, Preparation and characterization of activated carbons by one-step steam pyrolysis/activation from apricot stones, *Micropor. Mesopor. Mater.* 88 (2006) 126–134.
- [26] B.H. Hameed, I.A.W. Tan, A.L. Ahmad, Optimization of basic dye removal by oil palm fibre-based activated carbon using response surface methodology, *J. Hazard. Mater.* 158 (2008) 324–332.
- [27] D. Adinata, W.M.A.W. Daud, M.K. Aroua, Preparation and characterization of activated carbon from palm shell by chemical activation with K₂CO₃, *Bioresour. Technol.* 98 (2007) 145–149.
- [28] A.A. Amina, S.G. Badie, A.F. Nady, Removal of methylene blue by carbons derived from peach stones by H₃PO₄ activation: batch and column studies, *Dyes Pigments* 76 (2008) 282–289.
- [29] N. Kannan, M.M. Sundaram, Kinetics and mechanism of removal of methylene blue by adsorption on various carbons—a comparative study, *Dyes Pigments* 51 (2001) 25–40.
- [30] F. Rozada, M. Otero, A. Moran, A.I. Garcia, Activated carbons from sewage sludge and discarded tyres: production and optimization, *J. Hazard. Mater.* 124 (2005) 181–191.
- [31] I. Langmuir, Constitution and fundamental properties of solids and liquids. I. Solids, *J. Am. Chem. Soc.* 38 (11) (1916) 2221.
- [32] M.K.B. Gratuio, T. Panyathanmaporn, R.A. Chumnanklang, N.b. Sirinuntawitaya, A. Dutta, Production of activated carbon from coconut shell: optimization using response surface methodology, *Bioresour. Technol.* 99 (2008) 4887–4895.
- [33] IUPAC, IUPAC manual of symbols and terminology, *Pure Appl. Chem.* 31 (1972) 587.
- [34] J. Guo, A.C. Lua, Characterization of adsorbent prepared from oil-palm shell by CO₂ activation for removal of gaseous pollutants, *Mater. Lett.* 55 (2002) 334–339.
- [35] G.H. Oh, C.H. Yun, C.R. Park, Role of KOH in the one-stage KOH activation of cellulosic biomass, *Carbon Sci.* 4 (4) (2003) 180–184.
- [36] M. Olivares-Marín, C. Fernandez-Gonzalez, A. Macias-Garcia, V. Gomez-Serrano, Preparation of activated carbons from cherry stones by activation with potassium hydroxide, *Appl. Surf. Sci.* 252 (2006) 5980–5983.
- [37] A.C. Lua, T. Yang, Effect of activation temperature on the textural and chemical properties of potassium hydroxide activated carbon prepared from pistachio-nut shell, *J. Colloid Interface Sci.* 274 (2004) 594–601.